In Situ Analysis of Spatial Relationships between Proteins of the Nuclear Pore Complex

Marc Damelin and Pamela A. Silver
Department of Biological Chemistry and Molecular Pharmacology, Harvard Medical School and the Dana-Farber Cancer Institute, Boston, Massachusetts 02115 USA

ABSTRACT Macromolecular transport between the nucleus and cytoplasm occurs through the nuclear pore complexes (NPCs). The NPC in the budding yeast *Saccharomyces cerevisiae* is a 60-MDa structure embedded in the nuclear envelope and composed of ~30 proteins, termed nucleoporins or nups. Here we present a large-scale analysis of spatial relationships between nucleoporins using fluorescence resonance energy transfer (FRET) in living yeast cells. Energy transfer was measured in a panel of strains, each of which coexpresses the enhanced cyan and yellow fluorescent proteins as fusions to distinct nucleoporins. With this approach, we have determined 13 nucleoporin pairs yielding FRET signals. Independent experiments are consistent with the FRET results: Nup120 localization is perturbed in the *nic96–1* mutant, as is Nup82 localization in the *nup116*Δ mutant. To better understand the spatial relationship represented by an in vivo FRET signal, we have investigated the requirements of these signals. We demonstrate that in one case FRET signal is lost upon insertion of a short spacer between the nucleoporin and its enhanced yellow fluorescent protein label. We also show that the Nup120 FRET signals depend on whether the fluorescent moiety is fused to the N- or C-terminus of Nup120. Combined with existing data on NPC structure, the FRET pairs identified in this study allow us to propose a refined molecular model of the NPC. We suggest that the approach may serve as a prototype for the in situ study of other large macromolecular complexes.

INTRODUCTION

Understanding the organization of large macromolecular complexes is critical to dissecting their function. We have undertaken studies of one such structure in the cell, the nuclear pore complex (NPC), the centerpiece of the transport system between the nucleus and cytoplasm.

The compartmentalization of the eukaryotic cell into the nucleus and cytoplasm provides a means of regulating many cellular processes such as signal transduction, gene expression, and cell division (Nigg, 1997). All macromolecular transport between these compartments is thought to occur through the NPCs (Corbett and Silver, 1997; Davis, 1995).

The low-resolution structure of the NPC has been elucidated by electron cryomicroscopy and is marked by eightfold rotational symmetry (reviewed in Stoffler et al., 1999). Vertebrate and yeast NPCs have conserved structural domains such as the inner spoke ring, the cytoplasmic fibrils, and the nuclear basket (Yang et al., 1998). Vertebrate NPCs are ~125 MDa and measure ~120 nm in diameter and ~210 nm end-to-end; the corresponding values for yeast NPCs are 60 MDa, 100 nm, and 175 nm (Fahrenkrog et al., 1998).

The yeast NPC is composed of ~30 proteins termed nucleoporins or nups, each present in multiple copies (Rout et al., 2000). Most nucleoporins are present on the cytoplasmic and nuclear faces of the NPC, as determined by immunoelectron microscopy; however, some nucleoporins have asymmetric localization, with interesting implications for their function in translocation. Subcomplexes of nucleoporins have been isolated and characterized to varying degrees. Perhaps best characterized is the Nup84 subcomplex: interactions within the subcomplex have been identified by mass spectrometry, and the purified subcomplex has been imaged by electron microscopy (Rappsilber et al., 2000; Siniossoglou et al., 1996, 2000; Lutzmann et al., 2002).

The determination of the molecular organization of the NPC will be crucial to understanding the mechanism of nucleocytoplasmic translocation. At the minimum, translocation involves interactions between cargo-binding karyopherins and the NPC, with directionality conferred by the compartmentalized control of karyopherin-cargo interactions by the Ran GTPase (Mattaj and Englmeier, 1998; Ohno et al., 1998). Individual karyopherin-nucleoporin interactions would be more informative if placed in the context of the entire NPC. However, the organization of the NPC is difficult to analyze, as with any complex of this size. Because of the limitations of in vitro experiments in this context, we have pursued in vivo studies of NPC structural organization.

Spatial relationships between proteins can be analyzed in living cells by measuring fluorescence resonance energy transfer (FRET) between the enhanced cyan and yellow fluorescent proteins (ECFP and EYFP) (Tsien, 1998) expressed as fusions to proteins of interest. If the target proteins are close in space and bring the fluorophores in proximity, energy transfer from ECFP to EYFP can be detected by exciting ECFP and observing both increased EYFP emission and decreased ECFP emission. In general,

Submitted May 28, 2002, and accepted for publication July 22, 2002.

Address reprint requests to Dr. Pamela A. Silver, Department of Biological Chemistry and Molecular Pharmacology, Harvard Medical School and the Dana-Farber Cancer Institute, 1 Jimmy Fund Way, Boston, MA 02115. Tel.: 617-632-5102; Fax: 617-632-5103; E-mail: pamela_silver@dfci.harvard.edu.

0006-3495/02/12/3626/11 $2.00

energy transfer will occur only when the donor and acceptor are very close in space and in a particular relative orientation, making FRET a highly sensitive method (Clegg, 1996; Stryer, 1978). Green fluorescent protein (GFP)-based FRET has been applied in many experimental systems to study protein interactions as well as to measure local calcium concentrations, phosphorylation kinetics, protein cleavage kinetics, and other processes (Damelin and Silver, 2000; Day, 1998; Heim and Tsien, 1996; Mahajan et al., 1998; Miyawaki et al., 1997; Mochizuki et al., 2001; Jiang and Sorkin, 2002; Majoul et al., 2001, 2002; Warren et al., 2002; Sato et al., 2002; Immink et al., 2002; Ting et al., 2001; Weiss et al., 2001; Wilson et al., 2002; Ruiz-Velasco and Ikeda, 2001; Truong et al., 2001).

For the ECFP-EYFP pair, the interfluorophore distance corresponding to 50% FRET efficiency, termed the Forster radius R_o, is 49–52 Å (Tsien, 1998). FRET efficiency is proportional to the inverse sixth power of interfluorophore distance, and thus the Forster radius for a given FRET pair is an indication of the distances that can be detected by FRET. Therefore it is likely that ECFP-EYFP FRET signals in living cells represent an interfluorophore distance of not more than 50–60 Å. Because the fluorophores are buried inside the fluorescent proteins, this distance corresponds to a maximum separation between the ECFP and EYFP molecules themselves of 25–35 Å.

The ease of genetic manipulation in yeast allows the implementation of FRET in screening extensive sets of protein pairs (Damelin and Silver, 2000). In this study, we have used a FRET assay to investigate the structural organization of the yeast NPC. We have defined spatial relationships for 13 pairs of nucleoporins and have applied the data to generate a refined molecular model of the NPC. This study is distinct from our previous work (Damelin and Silver, 2000), in which we investigated interactions between proteins moving through the NPC and the nucleoporins; those results allowed us to analyze nuclear transport pathways but not the organization of the NPC. Our current results demonstrate that the approach can be used to probe the structural organization of multiprotein complexes. Consequently, this type of large-scale analysis has implications for studies of other macromolecular complexes whose structures are not known.

MATERIALS AND METHODS

Plasmid construction

The cassettes pRS304-ECFP-3′UTR (pPS1890) and pRS306-EYFP-3′UTR (pPS1891) and most *NUP-EYFP* plasmids have been described (Damelin and Silver, 2000). In these cases, ECFP or EYFP was fused to the C-terminus of the targeted gene. The vectors lack a yeast autonomous replication sequence and must integrate into the genome to be propagated. DNA encoding a C-terminal fragment of a given *NUP* gene was amplified by PCR from genomic DNA and cloned into pPS1890 and pPS1891. Each plasmid is linearized at a unique restriction site in the *NUP* fragment to target genomic integration to the *NUP* locus. Gene duplication is avoided because the plasmid contains only a small fragment of the *NUP* gene.

To generate pRS304-*ECFP-NUP120* (pPS2704), with ECFP fused to the N-terminus of *NUP120*, the 1-kb genomic fragment upstream of the *NOP1* gene, *ECFP*, and a 500-bp fragment of the 5′ end of *NUP120* were inserted into pRS304.

For the linker studies, a duplex oligonucleotide encoding 15 consecutive proline residues with an Ala-Arg-Ala flanking sequence on both sides was cloned into *NUP53-EYFP* (pPS1906), yielding pRS306-*NUP53-Pro*$_{(15)}$-*EYFP* (pPS2705), and into *NLS-ECFP-EYFP* (pPS1889), yielding pRS316-*NLS-ECFP-Pro*$_{(15)}$-*EYFP* (pPS2706). To generate pRS316-*NLS-ECFP-α−spectrin-EYFP* (pPS2707), DNA encoding residues 50–158 of α-spectrin (kindly provided by D. Speicher, Wistar Institute, Philadelphia, PA) was amplified by PCR, cloned into pCR-Blunt (Invitrogen, Carlsbad, CA) and then into pPS1889.

Yeast strains

The wild-type strain is the haploid FY23 in the S288C background (Winston et al., 1995). Yeast strains were transformed with the lithium acetate method. Individual transformants were checked for expression of ECFP- and EYFP-fusion proteins by microscopy and by immunoblotting with α-GFP antibody. We first generated a panel of Nup-EYFP strains (see Results and Damelin and Silver, 2000). We then transformed each Nup-EYFP strain with each of the other *NUP-ECFP* plasmids to generate 162 double-labeled strains. The Nup-EYFP strains were also transformed with *ECFP-NUP120* to generate 12 additional double-labeled strains. In all cases, several transformants were examined under the microscope for coexpression of the two fusions. For certain nucleoporin pairs, only some transformants coexpressed both fusions, but these cells still grew at the wild-type rate (data not shown). For all strains showing a FRET signal, PCR analysis was used to confirm integration of DNA encoding EYFP and ECFP at the correct *NUP* loci. Immunoblot analysis with α-GFP antibody was used to check coexpression of the fusion proteins. In 20 cases, none of the transformants that were examined coexpressed both fusions; these ECFP/EYFP pairs were Nup1/Nup49, Nup49/Nup1, Nup1/Nup85, Nup85/Nup1, Nic96/Nup49, Nup49/Nic96, Nic96/Nup85, Nup85/Nic96, Nup188/Nup49, Nup49/Nup188, Nup59/Nup133, Nup49/Nup85, Nup59/Nup53, Nup1/Nup145, Nup59/Nup84, Nup59/Nup85, Nic96/Nup59, Nup1/Nic96, Nup59/Nup49, and Nup49/Nup82. Some of these pairs correspond to known genetic interactions (e.g., Nup59/Nup53) or physical interactions (e.g., Nup49/Nic96), but most do not. It is unclear whether a problem in strain construction generally reflects an interaction between the nucleoporins. Occasional expression problems are common in large-scale analyses.

To examine the localization of Nup-EYFP fusions when putative interacting nucleoporins were mutated, *NUP-EYFP* plasmids were introduced into mutant strains. The *nic96–1* strain (Grandi et al., 1995b) was transformed to generate *nic96–1 NUP120-EYFP* (PSY2161) and *nic96–1 NUP116-EYFP* (PSY2162). The *nup116*Δ strain SWY27 (Wente and Blobel, 1993) was first backcrossed to wild-type FY86 to produce PSY1634, a *nup116*Δ strain that is *ADE2+* and thus does not accumulate red pigment. PSY1634 was transformed to generate *nup116*Δ *NUP82-EYFP* (PSY2163) and *nup116*Δ *NIC96-EYFP* (PSY2164).

Microscopy

Cells were grown at 25°C to log phase in synthetic complete (SC) medium, transferred to slides, and examined immediately. Cells were observed with a Nikon Diaphot-300 epifluorescence microscope, a ×60 1.4 NA Plan-APO objective, and Nomarski optics or the following filter sets (Omega Optical, Brattleboro, VT): *CFP*, 440-nm/20-nm excitation filter, 455-nm longpass dichroic filter, 480-nm/30-nm emission filter; *YFP*, 500/25-nm excitation, 525-nm longpass, 545/35-nm emission; *FRET*, 440/20-nm ex-

citation, 455-nm longpass, 535/25-nm emission. Images were captured with a liquid-cooled CCD camera (Photometrics, Tucson, AZ) equipped with a KAF-1400 chip, operated by the MetaMorph Imaging System (Universal Imaging Corp., West Chester, PA) and a model D122 shutter driver (UniBlitz, Rochester, NY).

The analysis of digitized microscope images allowed the selection of a certain region of the cell and thus optimized the signal-to-noise ratio. Digitized images of individual cells were captured first with the FRET filter set (1.5 s) and then with the CFP filter set (4 s). In cases where *FRET2* was calculated, an image with the YFP filter set (2 s) was captured after the FRET and before the CFP exposure. Settings for a given exposure were identical for all images being compared. Using the MetaMorph program, we highlighted the nuclear envelope and recorded the average pixel intensity per area in that region for the FRET, YFP, and CFP filter sets. The background intensity for each filter set was measured in empty fields and subtracted from the intensity in each cell.

Quantitative analysis was performed with a two- or three-filter set system. A simple ratio (Gordon et al., 1998; Hailey et al., 2002) was used for all comparisons of nucleoporin pairs, because in these cases the levels of ECFP and EYFP are consistent from cell to cell because of the genomic integration of the constructs. In this case the quantified value Q is defined by:

$$Q = Ff/Df, \quad (1)$$

where Ff is the signal intensity in the FRET filter set when both fluorophores are expressed, and Df is the intensity in the CFP filter set. All measurements are made with cells coexpressing ECFP and EYFP as fusions to different nucleoporins. The Ff/Df ratio is equivalent to the FRET/CFP ratio used previously (Damelin and Silver, 2000).

To identify positive FRET signals in nucleoporin pairs, Q was obtained for individual cells in each yeast strain. The rank sum test was used to statistically compare values for the various strains with a given Nup-ECFP, because ECFP contributes substantial cross-talk signal. Because of the cell-by-cell normalization of intensities, analysis of 12–15 cells per strain was sufficient to generate statistically significant data. The Ff/Df ratios for the cells in a given strain were averaged to yield the mean ratio. The mean ratios shown in Table 1 are normalized within each set of Nup-ECFP strains such that the average for the background strains is 1. This normalization is meant to facilitate data analysis and is permissible because Q values are not absolute.

The *FRET2* calculation (Gordon et al., 1998) was used in the linker studies based on nuclear localization signal (NLS)-ECFP-EYFP. In this case additional corrections are needed because these proteins are overexpressed (in contrast to the nucleoporin fusions) and because the expression levels from the plasmids fluctuate significantly from cell to cell. In our setup, there is no ECFP signal in the YFP filter set (i.e., $Ad = 0$) or EYFP signal in the CFP filter set (i.e., $Da = 0$). Thus, Eq. 13b from Gordon et al. (1998) reduces to:

$$FRET2 = \frac{Ff - Df(Fd/Dd) - Af(Fa/Aa)}{Ff - Df[(Fd/Dd) - G] - Af(Fa/Aa)}, \quad (2)$$

where Ff and Df are defined as above; Af is the signal intensity in the YFP filter set when both fluorophores are expressed; Fd and Dd are the signal intensities in the FRET and CFP filter sets, respectively, when only the ECFP fluorophore is expressed; Fa and Aa are the signal intensities in the FRET and YFP filter sets, respectively, when only the EYFP fluorophore is expressed; and G is a constant. Fd/Dd was measured with NLS-ECFP, and Fa/Aa was measured with NLS-EYFP. G was estimated to be 4, and varying G had little effect on the final *FRET2* values, as previously noted (Gordon et al., 1998).

TABLE 1 Quantitative analysis of FRET signals

ECFP fusion*	EYFP fusion†	Significance‡	Interaction§	Other ranges¶
Nup53	Nic96	$p < 0.005$	1.35	0.93–1.06
Nic96	Nup53	$p < 0.005$	1.17	0.96–1.02
Nup116	Nup82	$p < 0.001$	1.22	0.95–1.07
Nup82	Nup116	$p < 0.005$	1.20	0.91–1.11
Nup1	Nup188	$p < 0.025$	1.22	0.88–1.06
Nup188	Nup1	$p < 0.005$	1.17	0.94–1.04
Nup133	Nup188	$p < 0.005$	1.17	0.96–1.04
Nup188	Nup133	$p < 0.025$	1.14	0.96–1.03
Nup145C	Nup85	$p < 0.025$	1.14	0.93–1.06
Nup85	Nup145C	$p < 0.010$	1.33	0.88–1.16
Nup82	Nup120	$p < 0.025$	1.17	0.95–1.05
Nup120	Nup82	$p < 0.005$	1.23	0.93–1.07
ECFP-Nup120	Nup145C	$p < 0.005$	1.18	0.89–1.06
ECFP-Nup120	Nup188	$p < 0.001$	1.23	0.89–1.06
Nup84	Nup49	$p < 0.005$	1.40	0.91–1.06
Nup85	Nup49	$p < 0.010$	1.29	0.88–1.14
Nup188	Nup116	$p < 0.005$	1.25	0.94–1.04
Nup120	Nic96	$p < 0.025$	1.13	0.96–1.05
Gle1	Nup145C	$p < 0.005$	1.21	0.95–1.05

*Unless otherwise noted (for ECFP-Nup120), ECFP was fused to the C-terminus of the nucleoporin.
†EYFP was fused to the C-terminus of each nucleoporin listed.
‡The p value from the rank sum test that is true for all comparisons of the interacting pair and the other pairs with the same Nup-ECFP. Every p value indicates the significance of the interaction.
§Mean ratio for the interacting pair (see Materials and Methods for details).
¶Range of mean ratios for pairs expressing the same ECFP fusion and other EYFP fusions.

RESULTS

FRET defines spatial relationships between certain nucleoporin pairs

We first constructed 15 strains each expressing a functional fusion of EYFP to a particular nucleoporin (Nup-EYFP). DNA encoding EYFP was integrated into the genome at a *NUP* locus, generating an open reading frame that encodes a full-length Nup-EYFP fusion, with EYFP fused to the C-terminus of the nucleoporin. Each Nup-EYFP fusion replaced the endogenous nucleoporin and was the only copy of that nucleoporin in the cell. When viewed by fluorescence microscopy, each Nup-EYFP fusion localizes exclusively to the nuclear envelope. Immunoblot analysis confirms the expression of a full-length fusion migrating at the predicted size. We have previously described 13 Nup-EYFP strains: Nup1, Nup82, Nic96, Nup116, Nup145C, Nup120, Nup84, Nup85, Nup133, Nup53, Nup59, Nup188, and Nup2 (Damelin and Silver, 2000). Using the same method, we have generated Nup49-EYFP and Gle1-EYFP (data not shown). The functionality of each fusion was assessed by verifying localization at the nuclear envelope and expression of the full-length fusion under conditions in which the nucleoporin is essential for cell viability: Nup49, Gle1, Nup1, and Nup82 in wild type; Nup116, Nup145C, Nup120, Nup84, Nup85, and Nup133 in wild type at 37°C;

Nup53, Nup59, and Nup188 in *nup170*Δ; and Nup2 in *nup1–8*. All Nup-EYFP strains grow at the same rate as wild type. We could not generate functional fusions of EYFP to the C-terminus of Nsp1, Nup170, Nup159, Nup57, Nup100, or Nup42.

To study spatial relationships between nucleoporins in vivo, we generated yeast strains expressing pairwise combinations of labeled nucleoporins, one fused to ECFP and one to EYFP. A particular Nup-ECFP (also a C-terminal fusion) was expressed in the panel of Nup-EYFP strains, and the strains were analyzed for FRET. Direct comparisons were made only among the set of strains with a given Nup-ECFP, because ECFP contributes substantial cross-talk signal. For example, to identify FRET signals between Nup82 and the 14 other nucleoporins in the panel, DNA encoding ECFP was integrated into the genome at the *NUP82* locus in each Nup-EYFP strain. In the resulting cells, both fusions colocalized to the nuclear envelope and were expressed as full-length fusions, as shown for cells coexpressing Nup82-ECFP and Nup120-EYFP or Nup49-EYFP (Fig. 1, *A* and *B*).

When Nup82-ECFP and Nup120-EYFP are expressed in the same cell, a FRET signal is observed at the nuclear envelope (Fig. 1 *C*). In contrast, FRET signal is not observed in cells coexpressing Nup82-ECFP and Nup49-EYFP, or Nup82-ECFP and other Nup-EYFP fusions (Fig. 1 *C*). Cells expressing Nup82-ECFP and Nup116-EYFP also show a FRET signal.

The statistical significance of the FRET measurements was assessed by quantitative analysis. FRET signals were calculated with Eq. 1 (see Materials and Methods); in each cell the intensity at the nuclear envelope in the FRET channel was normalized by the intensity in the CFP channel. The ratios for 12–15 cells per strain were compared with the rank sum test. For instance, the rank sum test yielded $p < 0.025$ when Nup82/Nup120 was compared with each of the other pairs, demonstrating the significance of the measurement. Results for the Nup82/Nup116 pair are similar, with $p < 0.005$. Additionally, the ratios for the cells in each strain were averaged to yield the mean ratio. In this case, the mean ratios of Nup82/Nup120 and Nup82/Nup116 greatly exceeded the cluster of mean ratios of the other 12 pairs. For example, the Nup82/Nup120 value is 1.17, and the cluster values range from 0.95 to 1.05 (Table 1). Taken together with the visual observations (Fig. 1 *C*), these data indicate specific spatial relationships between two nucleoporin pairs involving Nup82.

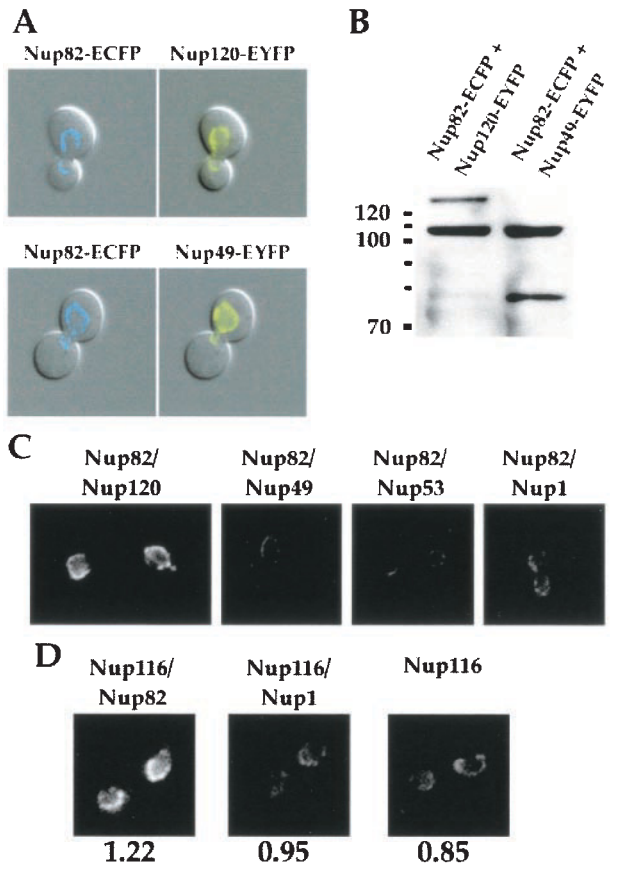

FIGURE 1 FRET signals between yeast nucleoporins. (*A*) Cells coexpressing Nup82-ECFP and Nup120-EYFP (*top panels*) or Nup82-ECFP and Nup49-EYFP (*bottom panels*) were viewed by fluorescence microscopy with Nomarski optics and filter sets for CFP (*left panels*) and YFP (*right panels*). (*B*) Whole-cell lysates of cells coexpressing Nup82-ECFP and Nup120-EYFP, or Nup82-ECFP and Nup49-EYFP, were resolved by SDS-polyacrylamide gel electrophoresis (SDS-PAGE) and immunoblotted with α-GFP antibody. (*C*) Cells coexpressing Nup82-ECFP and either Nup120-EYFP, Nup49-EYFP, Nup53-EYFP, or Nup1-EYFP were viewed by fluorescence microscopy with the FRET filter set, which allows selective excitation of ECFP and monitoring of EYFP emission. (*D*) Cells coexpressing Nup116-ECFP and Nup82-EYFP, or Nup116-ECFP and Nup1-EYFP, or Nup116-ECFP alone were viewed with the FRET filter set. Below each image is the mean ratio for that strain (see Materials and Methods).

Large-scale FRET analysis of spatial relationships between nucleoporins

We extended the study to all nucleoporin combinations in the matrix. In total, FRET signal was observed for 13 pairs: Nup53/Nic96, Nup1/Nup188, Nup84/Nup49, Nup85/Nup49, Nup145C/Nup85, Nup133/Nup188, Nup188/Nup116, Nup120/Nic96, Gle1/Nup145C, Nup82/Nup116, and Nup82/Nup120, and from experiments described below, Nup120/Nup145C and Nup120/Nup188. The results are presented in Fig. 2, and the quantitative analysis is summarized in Table 1. Importantly, all p values from the rank sum test are below the standard threshold of 0.05 and demonstrate the significance of the measurements. We performed photobleaching experiments as described (Damelin and Silver, 2000) and confirmed that the FRET signals were dependent on EYFP (data not shown). Consistent with our previous results (Damelin and Silver, 2000), the *Ff*/*Df* ratios for the background cluster are close to those for cells expressing only ECFP fusions in the cases we tested. For example, the mean ratio for Nup116-ECFP alone

EYFP fusion \ ECFP fusion	Nup1	Nup82	Nup84	Nup85	Nup145C	Nup116	Nup133	Nup53	Nup59	Nup188	Nic96	Nup49	Nup120-ECFP	ECFP-Nup120	Nup2	Gle1
Nup1										+ (1.17)						
Nup82						+ (1.22)							+ (1.23)			
Nup84																
Nup85					+ (1.14)											
Nup145C				+ (1.33)										+ (1.18)		+ (1.21)
Nup116		+ (1.20)								+ (1.25)						
Nup133										+ (1.14)						
Nup53											+ (1.17)					
Nup59																
Nup188	+ (1.22)						+ (1.17)							+ (1.23)		
Nic96								+ (1.35)					+ (1.13)			
Nup49			+ (1.40)	+ (1.29)												
Nup120		+ (1.17)														

FIGURE 2 Analysis of spatial relationships between NPC proteins. Each intersection of a Nup-ECFP column and a Nup-EYFP row represents a strain with two labeled nups. Nucleoporin pairs yielding a significant FRET signal are indicated with a + and the interaction value. The interaction value is relative to 1.0, the normalized average for the background strains; see Table 1 for more detail. In total, 174 strains were analyzed; 20 could not be constructed. ECFP and EYFP were fused to the C-terminus of nucleoporins in all cases except for ECFP-Nup120. The fusions in the three rightmost columns were used only as donors.

and Nup116-ECFP/Nup1-EYFP are similar, whereas that for Nup116-ECFP/Nup82-EYFP is much higher (Fig. 1 *D*).

The nucleoporin pairs yielding FRET signals in this study include several pairs of nucleoporins that previously have been shown to interact. The FRET data are consistent with independent biochemical evidence for four interactions: Nup116/Nup82 (Ho et al., 2000; Bailer et al., 2000), Nup53/Nic96 (Fahrenkrog et al., 2000), and Nup145C/Nup85 and Nup120/Nup145C (Rappsilber et al., 2000). Additionally, Nup1 copurifies with Nup170 (Kenna et al., 1996), which is in a subcomplex that has several genetic interactions with Nup188 (Nehrbass et al., 1996; Marelli et al., 1998), consistent with our observed FRET signal between Nup1 and Nup188. Several documented nucleoporin interactions were not detected in this study, because some of the nucleoporins could not be tagged with the fluorescent protein, and possibly because the particular conformations of some interactions are not amenable to the strict requirements for FRET.

Genetic analysis of nucleoporin pairs yielding FRET signal

To further substantiate the FRET data for certain nucleoporin pairs, we examined the localization of Nup-EYFP fusions in cells containing a mutation in the other nucleoporin. Nup120-EYFP shows a striking mislocalization in the *nic96–1* mutant, forming aggregates at one site on the nuclear envelope (Fig. 3 *A*). Other Nup-EYFP fusions, such as Nup116-EYFP and Nup188-EYFP, do not mislocalize in the same mutant (Fig. 3 *A*; data not shown), implying that the effect is specific to Nup120-EYFP. Moreover, Nic96–1 itself does not form aggregates at the nuclear envelope, although there is partial mislocalization to the cytoplasm (data not shown), suggesting that the Nup120-EYFP mislocalization in *nic96–1* is caused by a loss of interaction between Nup120 and Nic96.

We also found that Nup82-EYFP is substantially mislocalized to the cytoplasm in *nup116*Δ cells at 37°C compared with wild-type cells (Fig. 3 *C*). Nic96-EYFP does not mislocalize in the *nup116*Δ mutant (Fig. 3 *C*), showing that the effect is specific to Nup82-EYFP. However, we cannot explain the discrepancy between the mislocalization we observe and the intact localization of Nup82-GFP in a *nup116*Δ mutant, reported by Ho et al. (2000). Immunoblot analysis showed that the Nup82-EYFP and Nup120-EYFP fusions are expressed as full-length fusions in the mutants (Fig. 3, *B* and *D*), eliminating the possibility that the mislocalization is caused by proteolysis by-products. In sum-

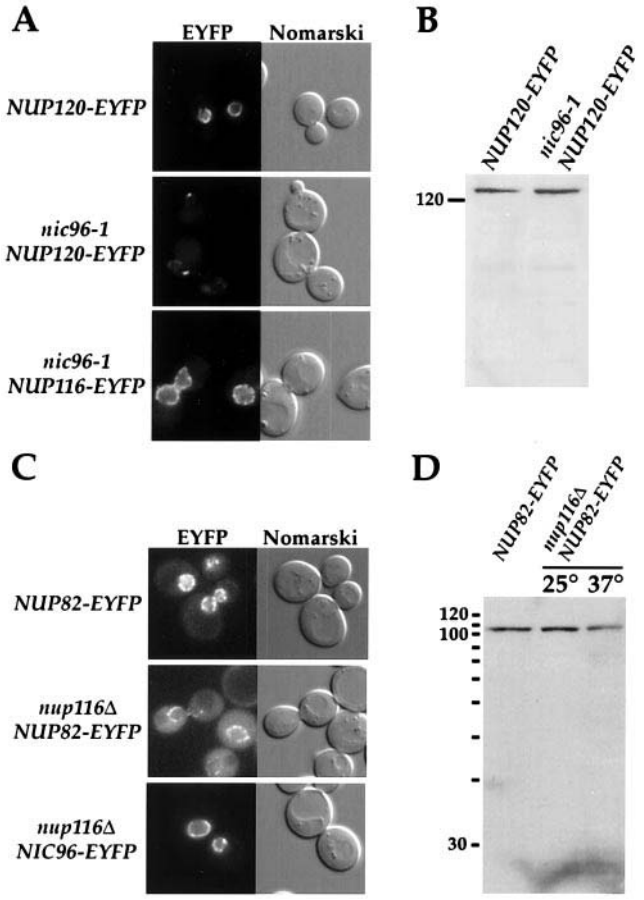

FIGURE 3 Mislocalization of nucleoporins caused by mutations in associated nucleoporins. (*A*) *NUP120-EYFP* cells, *nic96–1 NUP120-EYFP* cells, or *nic96–1 NUP116-EYFP* cells were grown to early log phase at 25°C and examined with the YFP filter set and Nomarski optics. (*B*) Whole-cell lysates of *NUP120-EYFP* cells or *nic96–1 NUP120-EYFP* cells were resolved by SDS-PAGE and immunoblotted with α-GFP antibody. The 120-kDa marker is indicated. (*C*) *NUP82-EYFP* cells, *nup116Δ NUP82-EYFP* cells, or *nup116Δ NIC96-EYFP* cells were grown to log phase at 25°C, shifted to 37°C for 2 h, and examined with the YFP filter set and Nomarski optics. (*D*) Whole-cell lysates of *NUP82-EYFP* cells at 37°C or *nup116Δ NUP82-EYFP* cells at 25°C and 37°C were resolved by SDS-PAGE and immunoblotted with α-GFP antibody.

mary, the two observed mislocalizations are consistent with the FRET data for these nucleoporin pairs.

Spatial requirements for in vivo FRET signals

Although an in vivo FRET signal cannot be interpreted to represent a direct interaction between the target proteins, it does indicate a certain relationship between the proteins. We performed several experiments to help determine the nature of the spatial relationship between a pair of target proteins yielding a FRET signal. First we examined the effect of moving the ECFP moiety from the C-terminus to the N-terminus of a nucleoporin, in this case Nup120. Originally ECFP was fused to the C-terminus of Nup120, as

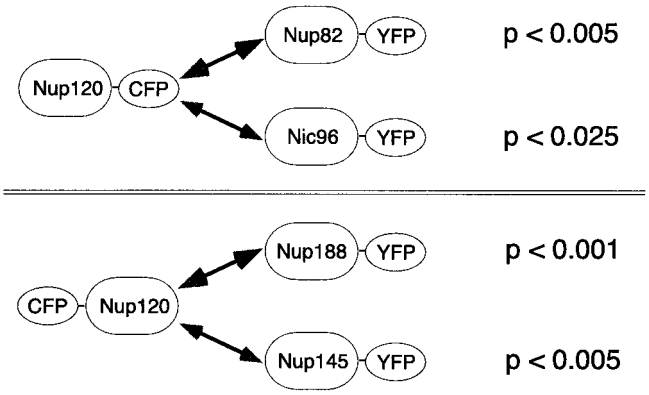

FIGURE 4 The specificity of in vivo FRET signals. Schematic diagram indicating the FRET signals observed for Nup120 when ECFP is fused to the C- versus N-terminus of Nup120. The *p* value is shown in each case.

described above. To see whether ECFP could instead be fused to the N-terminus of Nup120, DNA encoding ECFP was integrated into the genome at the *NUP120* locus to generate an open reading frame that encodes a full-length ECFP-Nup120 fusion. The *ECFP-NUP120* fusion replaces the endogenous *NUP120* and is the only copy of *NUP120* in the cell. The functionality of ECFP-Nup120 was confirmed by the viability of the cells at 37°C (where *NUP120* is required), the expression of a full-length fusion migrating at the expected size, as seen with immunoblot analysis, and its localization exclusively to the nuclear envelope (data not shown).

ECFP-Nup120 was expressed in the panel of Nup-EYFP strains, and the strains were analyzed with the FRET assay. Significant FRET signals were observed for cells expressing ECFP-Nup120 and Nup145C-EYFP and those expressing ECFP-Nup120 and Nup188-EYFP (Table 1). These nucleoporin pairs had not yielded FRET signals with ECFP fused to the C-terminus of Nup120. Additionally, the FRET signals originally observed with Nup120-ECFP (when paired with Nup82-EYFP and Nic96-EYFP) were no longer detected with ECFP-Nup120. The FRET signals for Nup120 therefore depend on whether ECFP is fused to the N- or C-terminus of the nucleoporin (Fig. 4). These results demonstrate the high degree of specificity of the in vivo FRET signals.

We further investigated the signal specificity by determining whether displacing EYFP with a short spacer affects the FRET signal. First we addressed this issue in more general terms by considering an ECFP-EYFP chimera and inserting the spacer between ECFP and EYFP. For these experiments we used the NLS-ECFP-EYFP construct in which the ECFP and EYFP are physically connected and yield a FRET signal (Damelin and Silver, 2000). In one case, a sequence of 15 consecutive proline residues, predicted to fold into a helix of ~45 Å in length (Creighton, 1984), was inserted between the ECFP and EYFP. In an-

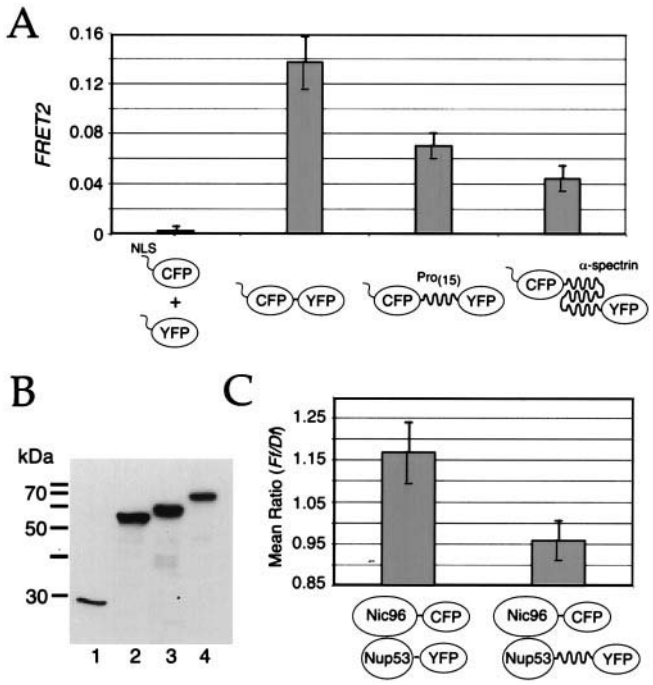

FIGURE 5 Short spacers disrupt FRET signals. (*A*) *FRET2* values for cells expressing either NLS-ECFP and NLS-EYFP, NLS-ECFP-EYFP, NLS-ECFP-Pro$_{(15)}$-EYFP, or NLS-ECFP-α-spectrin-EYFP. (*B*) Whole-cell lysates of the strains analyzed in *A* were resolved by SDS-PAGE and immunoblotted with α-GFP antibody. (*C*) Cells coexpressing Nic96-ECFP and either Nup53-EYFP or Nup53-Pro$_{(15)}$-EYFP were analyzed with the FRET assay.

other case, the spacer consisted of a compact domain of α-spectrin that forms a three-helix bundle with the N- and C-termini on opposite ends, separated by ~50 Å (Yan et al., 1993; Speicher and Marchesi, 1984). In the resulting NLS-ECFP-Pro$_{(15)}$-EYFP and NLS-ECFP-α-spectrin-EYFP fusions, both ECFP and EYFP are fluorescent (data not shown) and thus properly folded. Immunoblot analysis confirmed the expression of the fusions migrating at their predicted sizes (Fig. 5 *B*).

The FRET signal is significantly decreased in the presence of either spacer, as determined in cells expressing these constructs (Fig. 5 *A*). The rank sum test yielded $p < 0.001$ in comparisons of the NLS-ECFP-EYFP construct with each spacer construct, indicating that the differences are highly significant and that ECFP-EYFP FRET signals depend on interfluorophore distance. In these experiments, plasmid-based expression of ECFP and EYFP causes overexpression as well as substantial cell-to-cell variation in expression level, as opposed to the nucleoporin fusions for which the DNA encoding ECFP and EYFP is integrated into the genome. Thus FRET signal was calculated with Eq. 2 to yield *FRET2* values (see Materials and Methods); the *FRET2* calculation involves more corrections than *Q* used for the nucleoporin pairs (Eq. 1). It is important to note that changes in *FRET2* values are not proportional to changes in actual energy transfer (Gordon et al., 1998), so the extent of decrease in actual FRET cannot be determined from the data. This ambiguity also creates difficulty in interpreting the amount of FRET in the spacer constructs compared with background (ECFP + EYFP). It is not surprising that there is some FRET because the ECFP and EYFP are tethered by linkers that may not maintain a single conformation; for example, the polyproline linker may not be stabilized in a fully extended conformation in the context of this fusion.

To determine whether inserting a short spacer would also affect nucleoporin FRET signals, we examined the Nic96-Nup53 pair. The polyproline sequence was inserted between Nup53 and EYFP. The resulting Nup53- Pro$_{(15)}$-EYFP localizes exclusively to the nuclear envelope, and Nic96 coimmunoprecipitates with both Nup53- Pro$_{(15)}$-EYFP and Nup53-EYFP (data not shown). We compared cells coexpressing Nic96-ECFP and Nup53- Pro$_{(15)}$-EYFP with cells co-expressing Nic96-ECFP and Nup53-EYFP. The signal is significantly lower in the presence of the polyproline spacer, with $p < 0.001$ (Fig. 5C), and in fact is reduced to background levels (compare values in Table 1). Thus the FRET signal for this nucleoporin pair is sensitive to the insertion of a short spacer. The dependence of the FRET signals on the short spacer, and the specificity demonstrated by the Nup120 experiment, suggest that the FRET signals observed in this study correspond to nucleoporins separated by very small distances. In other words, even though FRET signals do not necessarily represent direct interactions, they define a spatial relationship between the respective target proteins in vivo.

DISCUSSION

The NPC is central to the transport of macromolecules between the cytoplasm and nucleus. We have studied the structural organization of the NPC in living yeast cells using FRET. With this approach we have defined spatial relationships for pairs of nucleoporins in the context of the intact NPC. Further characterization of the FRET method has demonstrated the specificity of the observed signals. Here we discuss the general applications of the technique and the implications of our results for the mechanism of nucleocytoplasmic transport.

Analysis of spatial relationships between nucleoporins with FRET

The results of this study, summarized in Fig. 2, provide several insights into the advantages of the FRET assay. The salient characteristic is specificity, as demonstrated by the relatively small number of interactions identified, the maintenance of the interactions when the ECFP and EYFP labels for a given FRET pair are swapped, and the strong dependence of FRET signals on ECFP-EYFP separation. Despite

this specificity, in vivo FRET analysis cannot be used to measure distances between the proteins or to infer direct interactions (Lakowicz, 1983; Gordon et al., 1998).

The large panel of nucleoporins provides an excellent set of internal controls for these experiments. Most in vivo FRET studies compare the putative interacting pair of target proteins with one or two noninteracting pairs. In contrast, in the current study, for a given Nup-ECFP fusion, we identified 10 or 11 control pairs that comprise the background cluster and one or two positive pairs yielding FRET signal. These results reiterate the specificity and significance of the FRET signals.

We have defined spatial relationships for 13 nucleoporin pairs. The combinations yielding FRET signals are evenly distributed in the panel: 14 of 16 nucleoporins were detected in interactions (Fig. 2). Thus the slight variations in Nup-EYFP intensities did not affect the results: nucleoporins with slightly lower intensity are well represented, and those with slightly higher intensity are not overrepresented. The specificity and distribution of the nucleoporin pairs imply that the FRET signals are genuine. We note that we do not detect FRET signal for any pair of nucleoporins that are predicted not to interact from previously published data, for example, between a nucleoporin located on the cytoplasmic face of the NPC and a nucleoporin located on the nuclear face.

In six of eight cases tested, the FRET signal between two nucleoporins is also observed when the ECFP and EYFP labels are swapped, as shown in Fig. 2 where the + signs are reflected across the diagonal. (In two untested cases the reciprocal strains could not be constructed; see Materials and Methods.) In the other two cases FRET signals are not detected in the reciprocal strains, possibly because the nucleoporins in those strains have different stoichiometries; FRET is favored with an excess of acceptor over donor (Clegg, 1996). For example, Nic96 is more abundant than Nup120 (Rout et al., 2000), and FRET signal is observed for Nup120-ECFP/Nic96-EYFP but not Nic96-ECFP/Nup120-EYFP. Even though the signal is not observed in both strains, the mislocalization of Nup120-EYFP in the *nic96–1* mutant is consistent with the FRET data.

An unavoidable consequence of the specificity of FRET is that some protein interactions are not detected with the assay; the absence of FRET signal between two nucleoporins cannot be interpreted to mean that those nucleoporins do not interact. In general, limitations in interpreting negative results are inherent in any method. The limitations for FRET result from the strict requirements for energy transfer (see Introduction). The linker experiments in Fig. 5 demonstrate the dependence of in vivo FRET signal on interfluorophore distance. Many of the nucleoporins are large, and interaction domains may be distant from the fluorescent proteins. The Nup120 experiment (Fig. 4) also addresses this point, because the observed FRET signals are dependent on the placement of ECFP on the N- versus C-terminus of Nup120. Thus extending the panel to include N-terminal fusions to all nucleoporins would increase the number of observed FRET signals. There would still be the likelihood of missing some interactions. However, we also note that two proteins that copurify in a subcomplex do not necessarily interact directly, as shown for some proteins in the Nup84 subcomplex (Rappsilber et al., 2000), in which case a FRET signal would not be expected.

The major implication of the above discussion is that the FRET signals represent very close associations, and possibly direct interactions, between the respective nucleoporins. We propose that this spatial relationship be called a FRET interaction to convey the understanding that the target proteins are closely associated in the physiological context of the cell, even though a direct interaction cannot be concluded.

The set of nucleoporin pairs yielding FRET signal is also constrained by our conservative interpretation of the data. When the mean ratios for all strains expressing a given Nup-ECFP are compared, most values form a cluster that establishes the background level (Table 1). We have listed only the nucleoporin pairs yielding signal above the background cluster, but the higher values within the cluster may also indicate FRET. Thus we infer 13 FRET-positive nucleoporin pairs but do not exclude the possibility of others; we expect that many nucleoporin interactions define the structure of the NPC. The purpose of this study was not to identify all of the nucleoporin pairs but to identify some not previously detected with other methods. Indeed, a valuable aspect of the FRET assay, based on its ability to probe interactions under physiological conditions, is to identify pairs of proteins that have a spatial relationship that may not be stable outside the context of the cell.

Four of the nucleoporin pairs we identified in this study represent previously documented interactions (see Results), but our attempts to detect interactions for some of the novel nucleoporin pairs by immunoprecipitation were unsuccessful. This might be explained by the intricate organization of the NPC; for example, many nucleoporin interactions are stable only in the context of larger subcomplexes (Schlaich et al., 1997; Lutzmann et al., 2002). These complications underscore the need for methods such as in vivo FRET analysis to study the structure of macromolecular complexes.

Refined molecular model of the NPC

Based on the spatial relationships between nucleoporins elucidated by our FRET analysis, we propose a refined molecular model of the yeast NPC that incorporates the 13 nucleoporin pairs from this study with existing data on the NPC. The purpose of this model is not to submit a definitive NPC structure but rather to suggest one way to assimilate all of the current information on the NPC, including the spatial relationships between 13 nucleoporin pairs as identified in

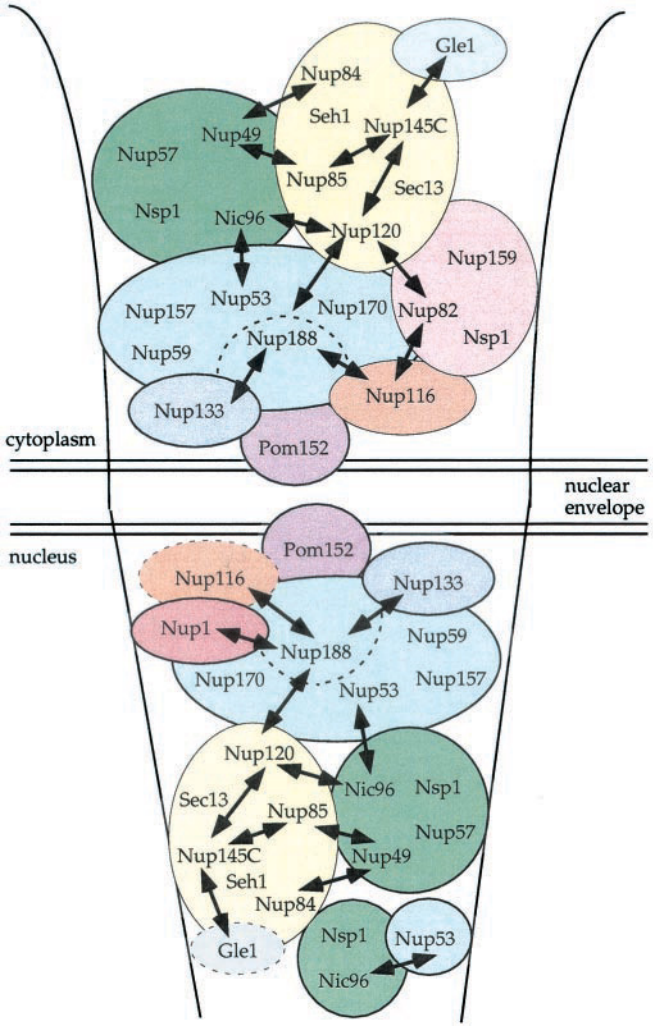

FIGURE 6 Molecular model of the yeast NPC. The black arrows represent nucleoporin pairs with a spatial relationship defined by FRET but do not necessarily imply direct interactions. Previously isolated subcomplexes are shown as discrete units (Belgareh et al., 1998; Hurwitz and Blobel, 1995; Grandi et al., 1993, 1995a; Siniossoglou et al., 1996; Marelli et al., 1998; Nehrbass et al., 1996). This arrangement was built upon the physical interaction between Nup188 and the membrane protein Pom152 (Nehrbass et al., 1996), which places Nup188 close to the nuclear envelope. For simplicity, we assume that the relationship between nucleoporin pairs exists wherever the nucleoporins colocalize in the NPC. The dotted lines for Nup116 and Gle1 on the nuclear face reflect that those nucleoporins are present mostly on the cytoplasmic face (Rout et al., 2000; Ho et al., 2000). The dotted line for Nup188 reflects the fact that several genetic interactions connect Nup188 to the Nup170 complex (Marelli et al., 1998; Nehrbass et al., 1996), even though a physical interaction has not been established.

this study. In the model, shown in Fig. 6, the black arrows represent FRET interactions between nucleoporins and thus imply the close association of those nucleoporins in the context of the structure (but not necessarily direct interactions). Individual nucleoporins and subcomplexes that have been treated as discrete units are now linked to one another in a cohesive network. The model includes 23 of the ~30 nucleoporins. Fig. 6 shows one of the eight subunits of the rotationally symmetric NPC. We note that some nucleoporins may be mobile within the NPC (Nakielny et al., 1999), but that has not been proposed for any of the nucleoporins in our panel.

Our model of the NPC builds upon the one proposed by Rout et al. (2000), which is based on the locations of individual nucleoporins by immunoelectron microscopy. The interpretation of the location analysis is limited in terms of gaining insight into nucleoporin function for two reasons: 1) many nucleoporins are large filamentous proteins that cannot be localized to a point, and 2) the data actually represent the locations of the protein-A tags fused to each nucleoporin. In contrast, the FRET-based model considers the nucleoporins in a more functional context. The spatial relationships between nucleoporins comprise an essential aspect of understanding NPC structural organization yet are not included in the Rout model. The two models constitute complementary representations of the NPC.

Our model also allows the visualization of translocation pathways of receptor-cargo complexes through the pore. For example, the model has implications for the mechanism of mRNA export by showing the spatial relationships among several nucleoporins associated with this process. Nup116, the Nup82 subcomplex, the Nup84 subcomplex, and Gle1 all show defects in mRNA export when mutated (Siniossoglou et al., 1996; Heath et al., 1995; Aitchison et al., 1995; Gorsch et al., 1995; Murphy and Wente, 1996; Hurwitz and Blobel, 1995; Belgareh et al., 1998; Del Priore et al., 1996). We observe FRET signals between Nup116 and Nup82, Nup82 and Nup120, and Nup145C and Gle1. Soluble factors carrying heterogeneous nuclear ribonucleoparticles (hnRNPs) to the cytoplasm could move from one binding site to another along this pathway.

CONCLUSION

Our model of the NPC is based on nucleoporin pairs with a spatial relationship defined by FRET, as identified from the evaluation of over 100 nucleoporin pairs. FRET has revealed many novel relationships that have not been detected by standard approaches but are consistent with previously published data, reiterating the advantages of in situ analysis. FRET should be applicable to the study of many other large macromolecular complexes, including the machinery involved in transcription, RNA processing, DNA replication, and intracellular transport.

We are grateful to E. Hurt, J. Loeb, S. Wente, and R. Wozniak for providing the nucleoporin mutants, to D. Speicher for the α-spectrin clone, to E. Minet for helpful discussions, and to A. Brodsky, C. Cole, A. Corbett, J. Hood-DeGrenier, S. Sever, and J. Way for comments on the manuscript.

This work was supported by grants to P.A.S. from the National Institutes of Health and the Human Frontiers in Science Program. M.D. was sup-

ported by National Institutes of Health Training grants in Tumor Biology and Biophysics.

REFERENCES

Aitchison, J. D., G. Blobel, and M. P. Rout. 1995. Nup120p: a yeast nucleoporin required for NPC distribution and mRNA transport. *J. Cell Biol.* 131:1659–1675.

Bailer, S. M., C. Balduf, J. Katahira, A. Podtelejnikov, C. Rollenhagen, M. Mann, N. Pante, and E. Hurt. 2000. Nup116p associates with the Nup82p-Nsp1p-Nup159p nucleoporin complex. *J. Biol. Chem.* 275: 23540–23548.

Belgareh, N., C. Snay-Hodge, F. Pasteau, S. Dagher, C. N. Cole, and V. Doye. 1998. Functional characterization of a Nup159p-containing nuclear pore subcomplex. *Mol. Biol. Cell.* 9:3475–3492.

Clegg, R. M. 1996. Fluorescence resonance energy transfer. *In* Fluorescence Imaging Spectroscopy and Microscopy. X. F. Wang and B. Herman, editors. Wiley, New York. 179–252.

Corbett, A. H., and P. A. Silver. 1997. Nucleocytoplasmic transport of macromolecules. *Microbiol. Mol. Biol. Rev.* 61:193–211.

Creighton, T. E. 1984. Proteins: Structures and Molecular Properties. W. H. Freeman, New York.

Damelin, M., and P. A. Silver. 2000. Mapping interactions between nuclear transport factors in living cells reveals pathways through the nuclear pore complex. *Mol. Cell.* 5:133–140.

Davis, L. I. 1995. The nuclear pore complex. *Annu. Rev. Biochem.* 64: 865–896.

Day, R. N. 1998. Visualization of Pit-1 transcription factor interactions in the living cell nucleus by fluorescence resonance energy transfer microscopy. *Mol. Endocrinol.* 12:1410–1419.

Del Priore, V., C. A. Snay, A. Bahr, and C. N. Cole. 1996. The product of the *Saccharomyces cerevisiae* RSS1 gene, identified as a high-copy suppressor of the rat7–1 temperature-sensitive allele of the RAT7/NUP159 nucleoporin, is required for efficient mRNA export. *Mol. Biol. Cell.* 7:1601–1621.

Fahrenkrog, B., W. Huebner, A. Mandinova, N. Pante, W. Keller, and U. Aebi. 2000. The yeast nucleoporin Nup53p specifically interacts with Nic96p and is directly involved in nuclear protein import. *Mol. Biol. Cell.* 11:3885–3896.

Fahrenkrog, B., E. C. Hurt, U. Aebi, and N. Pante. 1998. Molecular architecture of the yeast nuclear pore complex: localization of Nsp1p subcomplexes. *J. Cell Biol.* 143:577–588.

Gordon, G. W., G. Berry, X. H. Liang, B. Levine, and B. Herman. 1998. Quantitative fluorescence resonance energy transfer measurements using fluorescence microscopy. *Biophys. J.* 74:2702–2713.

Gorsch, L. C., T. C. Dockendorff, and C. N. Cole. 1995. A conditional allele of the novel repeat-containing yeast nucleoporin RAT7/NUP159 causes both rapid cessation of mRNA export and reversible clustering of nuclear pore complexes. *J. Cell Biol.* 129:939–955.

Grandi, P., V. Doye, and E. C. Hurt. 1993. Purification of NSP1 reveals complex formation with 'GLFG' nucleoporins and a novel nuclear pore protein NIC96. *EMBO J.* 12:3061–3071.

Grandi, P., S. Emig, C. Weise, F. Hucho, T. Pohl, and E. C. Hurt. 1995a. A novel nuclear pore protein Nup82p which specifically binds to a fraction of Nsp1p. *J. Cell Biol.* 130:1263–1273.

Grandi, P., N. Schlaich, H. Tekotte, and E. C. Hurt. 1995b. Functional interaction of Nic96p with a core nucleoporin complex consisting of Nsp1p, Nup49p and a novel protein Nup57p. *EMBO J.* 14:76–87.

Hailey, D. W., T. N. Davis, and E. G. D. Muller. 2002. Fluorescence resonance energy transfer using color variants of GFP. *Methods Enzymol.* 351:34–49.

Heath, C. V., C. S. Copeland, D. C. Amberg, V. Del Priore, M. Snyder, and C. N. Cole. 1995. Nuclear pore complex clustering and nuclear accumulation of poly(A)+ RNA associated with mutation of the *Saccharomyces cerevisiae* RAT2/NUP120 gene. *J. Cell Biol.* 131:1677–1697.

Heim, R., and R. Y. Tsien. 1996. Engineering green fluorescent protein for improved brightness, longer wavelengths and fluorescence resonance energy transfer. *Curr. Biol.* 6:178–182.

Ho, A. K., T. X. Shen, K. J. Ryan, E. Kiseleva, M. A. Levy, T. D. Allen, and S. R. Wente. 2000. Assembly and preferential localization of Nup116p on the cytoplasmic face of the nuclear pore complex by interaction with Nup82p. *Mol. Cell. Biol.* 20:5736–5748.

Hurwitz, M. E., and G. Blobel. 1995. NUP82 is an essential yeast nucleoporin required for poly(A)+ RNA export. *J. Cell Biol.* 130:1275–1281.

Immink, R. G., T. W. Gadella, Jr., S. Ferrario, M. Busscher, and G. C. Angenent. 2002. Analysis of MADS box protein-protein interactions in living plant cells. *Proc. Natl. Acad. Sci. U.S.A.* 99:2416–2421.

Jiang, X., and A. Sorkin. 2002. Coordinated traffic of Grb2 and Ras during epidermal growth factor receptor endocytosis visualized in living cells. *Mol. Biol. Cell.* 13:1522–1535.

Kenna, M. A., J. G. Petranka, J. L. Reilly, and L. I. Davis. 1996. Yeast N1e3p/Nup170p is required for normal stoichiometry of FG nucleoporins within the nuclear pore complex. *Mol. Cell. Biol.* 16:2025–2036.

Lakowicz, J. R. 1983. Energy transfer. *In* Principles of Fluorescence Spectroscopy. Plenum, New York. 305–341.

Lutzmann, M., R. Kunze, A. Buerer, U. Aebi, and E. Hurt. 2002. Modular self-assembly of a Y-shaped multiprotein complex from seven nucleoporins. *EMBO J.* 21:387–397.

Mahajan, N. P., K. Linder, G. Berry, G. W. Gordon, R. Heim, and B. Herman. 1998. Bcl-2 and Bax interactions in mitochondria probed with green fluorescent protein and fluorescence resonance energy transfer. *Nat. Biotechnol.* 16:547–552.

Majoul, I., M. Straub, R. Duden, S. W. Hell, and H. D. Soling. 2002. Fluorescence resonance energy transfer analysis of protein-protein interactions in single living cells by multifocal multiphoton microscopy. *J. Biotechnol.* 82:267–277.

Majoul, I., M. Straub, S. W. Hell, R. Duden, and H. D. Soling. 2001. KDEL-cargo regulates interactions between proteins involved in COPI vesicle traffic: measurements in living cells using FRET. *Dev. Cell.* 1:139–153.

Marelli, M., J. D. Aitchison, and R. W. Wozniak. 1998. Specific binding of the karyopherin Kap121p to a subunit of the nuclear pore complex containing Nup53p, Nup59p, and Nup170p. *J. Cell Biol.* 143: 1813–1830.

Mattaj, I. W., and L. Englmeier. 1998. Nucleocytoplasmic transport: the soluble phase. *Annu. Rev. Biochem.* 67:265–306.

Miyawaki, A., J. Llopis, R. Heim, J. M. McCaffery, J. A. Adams, M. Ikura, and R. Y. Tsien. 1997. Fluorescent indicators for Ca^{2+} based on green fluorescent proteins and calmodulin. *Nature.* 388:882–887.

Mochizuki, N., S. Yamashita, K. Kurokawa, Y. Ohba, T. Nagai, A. Miyawaki, and M. Matsuda. 2001. Spatio-temporal images of growth-factor-induced activation of Ras and Rap1. *Nature.* 411:1065–1068.

Murphy, R., and S. R. Wente. 1996. An RNA-export mediator with an essential nuclear export signal. *Nature.* 383:357–360.

Nakielny, S., S. Shaikh, B. Burke, and G. Dreyfuss. 1999. Nup153 is an M9-containing mobile nucleoporin with a novel Ran-binding domain. *EMBO J.* 18:1982–1995.

Nehrbass, U., M. P. Rout, S. Maguire, G. Blobel, and R. W. Wozniak. 1996. The yeast nucleoporin Nup188p interacts genetically and physically with the core structures of the nuclear pore complex. *J. Cell Biol.* 133:1153–1162.

Nigg, E. A. 1997. Nucleocytoplasmic transport: signals, mechanisms and regulation. *Nature.* 386:779–787.

Ohno, M., M. Fornerod, and I. W. Mattaj. 1998. Nucleocytoplasmic transport: the last 200 nanometers. *Cell.* 92:327–336.

Rappsilber, J., S. Siniossoglou, E. C. Hurt, and M. Mann. 2000. A generic strategy to analyze the spatial organization of multi-protein complexes by cross-linking and mass spectrometry. *Anal. Chem.* 72:267–275.

Rout, M. P., J. D. Aitchison, A. Suprapto, K. Hjertaas, Y. Zhao, and B. T. Chait. 2000. The yeast nuclear pore complex: composition, architecture, and transport mechanism. *J. Cell Biol.* 148:635–651.

Ruiz-Velasco, V., and S. R. Ikeda. 2001. Functional expression and FRET analysis of green fluorescent proteins fused to G-protein subunits in rat sympathetic neurons. *J. Physiol.* 537:679–692.

Sato, M., T. Ozawa, K. Inukai, T. Asano, and Y. Umezawa. 2002. Fluorescent indicators for imaging protein phosphorylation in single living cells. *Nat. Biotechnol.* 20:287–294.

Schlaich, N. L., M. Haner, A. Lustig, U. Aebi, and E. C. Hurt. 1997. In vitro reconstitution of a heterotrimeric nucleoporin complex consisting of recombinant Nsp1p, Nup49p, and Nup57p. *Mol. Biol. Cell.* 8:33–46.

Siniossoglou, S., M. Lutzmann, H. Santos-Rosa, K. Leonard, S. Mueller, U. Aebi, and E. Hurt. 2000. Structure and assembly of the Nup84p complex. *J. Cell Biol.* 149:41–54.

Siniossoglou, S., C. Wimmer, M. Rieger, V. Doye, H. Tekotte, C. Weise, S. Emig, A. Segref, and E. C. Hurt. 1996. A novel complex of nucleoporins, which includes Sec13p and a Sec13p homolog, is essential for normal nuclear pores. *Cell.* 84:265–275.

Speicher, D. W., and V. T. Marchesi. 1984. Erythrocyte spectrin is comprised of many homologous triple helical segments. *Nature.* 311: 177–180.

Stoffler, D., B. Fahrenkrog, and U. Aebi. 1999. The nuclear pore complex: from molecular architecture to functional dynamics. *Curr. Opin. Cell Biol.* 11:391–401.

Stryer, L. 1978. Fluorescence energy transfer as a spectroscopic ruler. *Annu. Rev. Biochem.* 47:819–846.

Ting, A. Y., K. H. Kain, R. L. Klemke, and R. Y. Tsien. 2001. Genetically encoded fluorescent reporters of protein tyrosine kinase activities in living cells. *Proc. Natl. Acad. Sci. U.S.A.* 98:15003–15008.

Truong, K., A. Sawano, H. Mizuno, H. Hama, K. I. Tong, T. K. Mal, A. Miyawaki, and M. Ikura. 2001. FRET-based in vivo Ca^{2+} imaging by a new calmodulin-GFP fusion molecule. *Nat. Struct. Biol.* 8:1069–1073.

Tsien, R. 1998. The Green Fluorescent Protein. *Annu. Rev. Biochem.* 67:509–544.

Warren, D. T., P. D. Andrews, C. W. Gourlay, and K. R. Ayscough. 2002. Sla1p couples the yeast endocytic machinery to proteins regulating actin dynamics. *J. Cell Sci.* 115:1703–1715.

Weiss, T. S., C. E. Chamberlain, T. Takeda, P. Lin, K. M. Hahn, and M. G. Farquhar. 2001. Galpha i3 binding to calnuc on Golgi membranes in living cells monitored by fluorescence resonance energy transfer of green fluorescent protein fusion proteins. *Proc. Natl. Acad. Sci. U.S.A.* 98:14961–14966.

Wente, S. R., and G. Blobel. 1993. A temperature-sensitive NUP116 null mutant forms a nuclear envelope seal over the yeast nuclear pore complex thereby blocking nucleocytoplasmic traffic. *J. Cell Biol.* 123: 275–284.

Wilson, M. C., D. Meredith, and A. P. Halestrap. 2002. Fluorescence resonance energy transfer studies on the interaction between the lactate transporter MCT1 and CD147 provide information on the topology and stoichiometry of the complex in situ. *J. Biol. Chem.* 277:3666–3672.

Winston, F., C. Dollard, and S. L. Ricupero-Hovasse. 1995. Construction of a set of convenient *Saccharomyces cerevisiae* strains that are isogenic to S288C. *Yeast.* 11:53–55.

Yan, Y., E. Winograd, A. Viel, T. Cronin, S. C. Harrison, and D. Branton. 1993. Crystal structure of the repetitive segments of spectrin. *Science.* 262:2027–2030.

Yang, Q., M. P. Rout, and C. W. Akey. 1998. Three-dimensional architecture of the isolated yeast nuclear pore complex: functional and evolutionary implications. *Mol. Cell.* 1:223–234.